

Geophysical Research Letters®

RESEARCH LETTER

10.1029/2021GL096362

Key Points:

- The summer North Atlantic Oscillation is found to become predictable in the recent decades
- March North Atlantic jet strength is the key predictor for the seasonal forecast of the summer North Atlantic Oscillation
- Stratosphere-troposphere dynamical coupling leads to this extended seasonal predictability of the summer North Atlantic Oscillation

Supporting Information:

Supporting Information may be found in the online version of this article.

Correspondence to:

L. Wang,
wanglei_ias@fudan.edu.cn

Citation:

Wang, L., & Ting, M. (2022). Stratosphere-troposphere coupling leading to extended seasonal predictability of summer North Atlantic Oscillation and boreal climate. *Geophysical Research Letters*, 49, e2021GL096362. <https://doi.org/10.1029/2021GL096362>

Received 26 SEP 2021

Accepted 10 JAN 2022

Author Contributions:

Conceptualization: Lei Wang, Mingfang Ting

Formal analysis: Lei Wang

Funding acquisition: Lei Wang, Mingfang Ting

Methodology: Lei Wang

Project Administration: Lei Wang

Writing – original draft: Lei Wang

Writing – review & editing: Lei Wang, Mingfang Ting

© 2022 The Authors.

This is an open access article under the terms of the [Creative Commons Attribution-NonCommercial License](https://creativecommons.org/licenses/by/4.0/), which permits use, distribution and reproduction in any medium, provided the original work is properly cited and is not used for commercial purposes.

Stratosphere-Troposphere Coupling Leading to Extended Seasonal Predictability of Summer North Atlantic Oscillation and Boreal Climate

Lei Wang^{1,2,3,4}  and Mingfang Ting⁴ 

¹Department of Atmospheric and Oceanic Sciences & Institute of Atmospheric Sciences, Fudan University, Shanghai, China, ²Shanghai Qi Zhi Institute, Shanghai, China, ³Innovation Center of Ocean and Atmosphere System, Zhuhai Fudan Innovation Research Institute, Zhuhai, China, ⁴Lamont-Doherty Earth Observatory, Columbia University, Palisades, NY, USA

Abstract The boreal summer climate is of significant societal importance and is trending toward increased risks of extreme climate events such as heatwaves. The summer North Atlantic Oscillation, as the primary mode of atmospheric variability in the northern hemisphere, has been long considered lacking predictability on seasonal time scales. Here we show that the summer North Atlantic Oscillation is predictable with a 2-month lead for the recent decades. The primary predictor is the March North Atlantic jet strength, which is correlated with the summer North Atlantic Oscillation index at a correlation coefficient of 0.66 over 1979–2018. Spring stratosphere-troposphere coupling plays a critical role in this extended predictability from spring to summer, in contrast to the common knowledge that this dynamical coupling is relatively inactive outside the winter season. These results may bring sound prospects for summer seasonal prediction of boreal climate that benefits the energy and public health sectors.

Plain Language Summary The summer climate in the northern hemisphere is of significant societal importance. Extreme climate events such as heatwaves occur more and more frequently under global warming. The summer North Atlantic Oscillation is a good representation of atmospheric motions in the North Atlantic region and can influence the atmospheric flow of the entire northern hemisphere. Scientists have not made accurate seasonal forecast of this mode and hence boreal summer climate. In this study, we discovered a key predictor in March whose signal can be transmitted by the stratosphere back to the summer surface to make the summer North Atlantic Oscillation predictable 2 months in advance. Our findings can help the society better prepared for the extreme summer climate in the northern hemisphere.

1. Introduction

The summer North Atlantic Oscillation (SNAO; see definitions in the data section) is the dominant mode of summer climate variability in the Euro-Atlantic region (Folland et al., 2009) and can influence surface climate over most extratropical regions in the northern hemisphere (Figure 1). A positive SNAO may increase the risk of extremely dry and hot weather conditions over the European coastal areas, most of North America, and as far as East Asia, whereas a negative SNAO may affect pan-Mediterranean regions, Eastern Canada, and Greenland (Figure 1). For example, the 2018 northern Europe summer heatwave was linked to an anomalously positive SNAO (Drouard et al., 2019), and another major heatwave hit most of the Mediterranean in 2019 summer during the negative phase of SNAO (Sousa et al., 2019). The affected regions in both summers are consistent with where SNAO is the most impactful (as indicated by the dark red and blue regions in Figure 1, respectively). Nevertheless, SNAO has been considered much less predictable than its winter counterpart on seasonal and longer time scales (Franzke & Woollings, 2011). Operational forecast systems can skilfully predict the winter North Atlantic Oscillation (NAO) with a 1-month lead (Scaife et al., 2014) and even with some skill up to 13 months in advance (Dunstone et al., 2016). Empirical models based on observations (Hall et al., 2017; Wang et al., 2017) also show strong predictability of winter NAO with a few months of lead time. It would be highly beneficial to society if SNAO can be predicted at a similar level, given the increasing risks of heatwaves under the warming climate. However, SNAO remains poorly understood and skillful predictions of SNAO are very limited in forecast models (Dunstone et al., 2018) with only marginal predictability in empirical models based on sea surface temperatures (Baker et al., 2019).

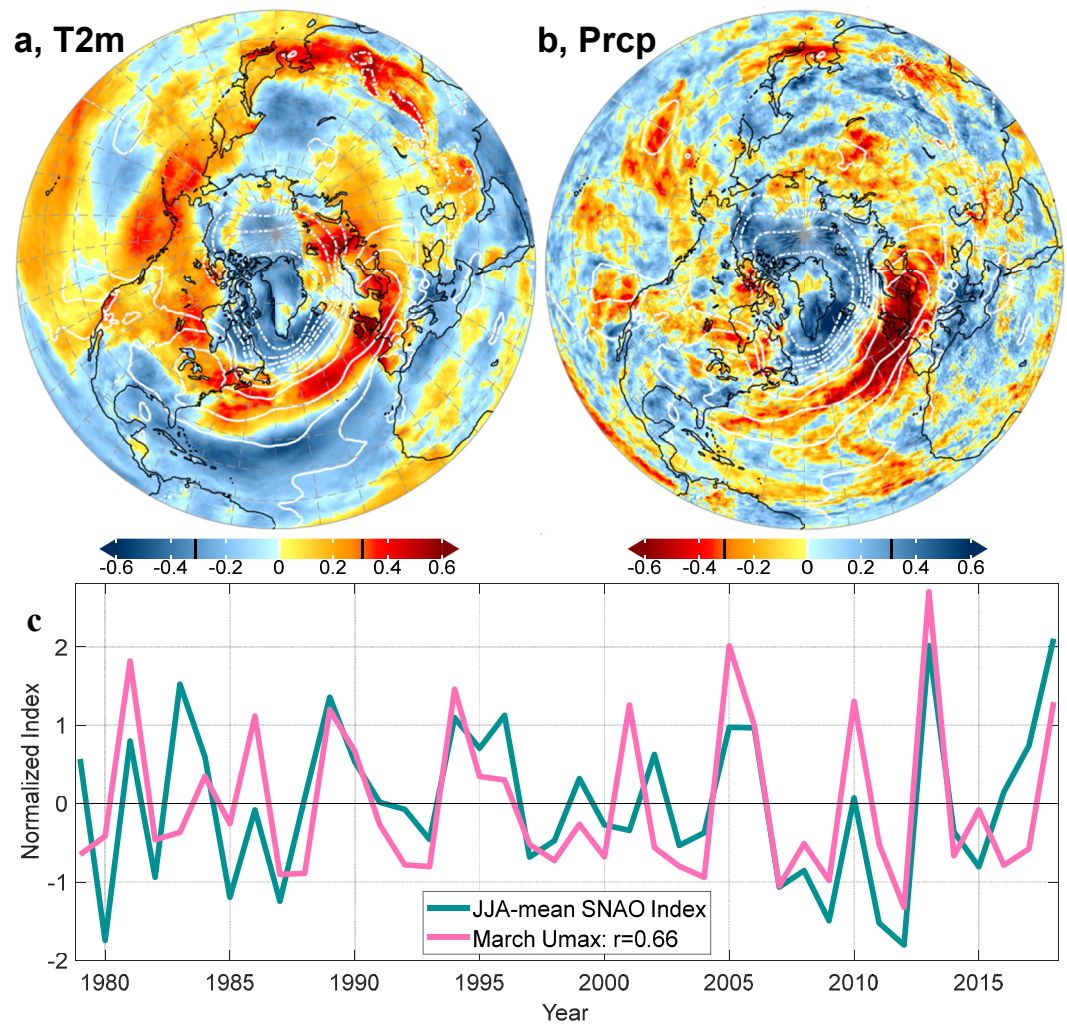


Figure 1. Summer surface climate associated with summer North Atlantic Oscillation (NAO). The ERA5 1979–2018 correlation between the June–July–August (JJA)–mean SNAO index and (a), 2 m temperature and (b), total precipitation, overlaid with the correlation between mean sea level pressure and the SNAO index (white contours with a 0.2 interval; positive in solid and negative in dashed). (c), time series of the JJA–mean SNAO index and March North Atlantic jet strength. Black lines on the colorbars indicate the 95% confidence level by a two-tailed t -test.

2. Methods

A multiple linear regression model (Kutner et al., 2005) is constructed to evaluate the predictability of the June–July–August (JJA) seasonal–mean NAO index (or SNAO, i.e., the predictand) and 12 potential spring predictors are considered based on their possible physical or dynamical linkages to SNAO. Many of the potential predictors are motivated by Hall et al. (2017), but the primary predictor, the March tropospheric barotropic jet strength, is the new predictor found in this manuscript. The tropospheric barotropic jet strength in the North Atlantic region is defined as the maximum within 20–65°N in the zonal wind averaged over 75°W–15°E and 100–1,000 hPa (denoted as U_{\max}). The vertical average is weighted by mass/pressure of each layer.

The optimal set of predictors are identified by a forward selection method based on hindcast skill (Kutner et al., 2005). The hindcast is obtained by fitting the regression model using the entire 40-year time series of the predictors and the predictand (Kutner et al., 2005). Having the highest correlation with the predictand, the March North Atlantic jet strength is chosen as the first predictor for SNAO. The other candidate predictors are added one by one to the regression model, and the predictor that boosts the hindcast skill most is identified as the second predictor. A potential predictor will be discarded to avoid co-linearity (Kutner et al., 2005) if it has a

correlation coefficient >0.6 with any of the existing predictors. This procedure is repeated for all potential predictors, resulting in a set of predictors that produces high hindcast skill (gray curve in Figure S1a in Supporting Information S1).

We use a strict two-fold cross-validation procedure (Kutner et al., 2005) to ensure the robustness of the model. The entire 40-year period of 1979–2018 is divided into two 20-year periods, that is, 1979–1998 and 1999–2018, and each time the regression model is estimated using one 20-year period and validated using the other 20-year period. Repeating the validation twice results in a two-fold cross-validated forecast for the entire 40-year period. Hindcast skill is usually higher than the cross-validated forecast skill for any given combination of predictors, and the regression model is considered robust if the forecast skill is close to the hindcast skill. The cross-validated forecast skill starts to separate with the hindcast skill from the fifth predictor (Figure S1a in Supporting Information S1). The first four predictors are then selected as the optimal set of predictors for the seasonal forecast of SNAO, including the March North Atlantic tropospheric barotropic jet strength (pink curve in Figure 1c), the eastern Indian Ocean rainfall, the North Atlantic SST, and the April Arctic sea ice extent (Figure S1b in Supporting Information S1). The last three indices are motivated by Hall et al. (2017) and taken as domain averages of the eastern Indian Ocean rainfall for the region $0\text{--}30^{\circ}\text{N}$ and $75\text{--}115^{\circ}\text{E}$, the North Atlantic SST for the region $35\text{--}45^{\circ}\text{N}$ and $70\text{--}40^{\circ}\text{W}$, and the Arctic sea ice extent in the Pacific sector, $120^{\circ}\text{E}\text{--}120^{\circ}\text{W}$ and $40\text{--}65^{\circ}\text{N}$.

3. Data

Data used in this study are from seven reanalysis datasets, including the ECMWF Interim Reanalysis (ERA-Interim; Dee et al., 2011), the ECMWF Reanalysis v5.1 (ERA5; Copernicus Climate Change Service, 2017), the ECMWF Coupled Climate Reanalyses of the 20th Century (CERA20C; Lalouaux et al., 2018), the NCEP-DOE AMIP-II Reanalysis (NCEP2; Kanamitsu et al., 2002), the Modern-Era Retrospective analysis for Research and Applications, version 2 (MERRA2; Collins et al., 2005), the Japanese 55-year Reanalysis (JRA-55; Kobayashi et al., 2015), and the NOAA-CIRES 20th Century Reanalysis (NOAA20CR; Slivinski et al., 2019). The pointwise SNAO index is defined here as the difference between the mean sea level pressure (MSLP) averaged over two domains: ($25^{\circ}\text{W}\text{--}5^{\circ}\text{E}$, $45\text{--}55^{\circ}\text{N}$) and ($52\text{--}22^{\circ}\text{W}$, $60\text{--}70^{\circ}\text{N}$), which are selected to cover the two nodes of the leading Empirical Orthogonal Function (EOF) pattern of the JJA MSLP within the North Atlantic region ($70^{\circ}\text{W}\text{--}50^{\circ}\text{E}$, $25\text{--}70^{\circ}\text{N}$; following Folland et al., 2009), as shown in Figures S2a–S2c in Supporting Information S1. This pointwise definition is more convenient for comparisons among different datasets or time periods than the principal component (PC)-based definition (Hurrell et al., 2003) and both produce consistent SNAO indices (Figures S2d–S2e in Supporting Information S1). The station-based definition (Hurrell, 1995), on the other hand, does not work well for SNAO due to the poleward shift of the jet stream and the associated centers of action, that is, the Icelandic Low and the Azores-Bermuda High, in summer relative to their winter positions (Folland et al., 2009). Therefore, the pointwise SNAO index is used throughout the manuscript.

4. Results

Variability of the winter NAO has been considered as interactions between the subtropical (or thermal-driven) jet and subpolar (or eddy-driven) jet in the North Atlantic (Gerber & Vallis, 2009). Unsurprisingly, NAO variability in other seasons shows similar behavior. A positive SNAO tends to be preceded in spring (March and April) by a strong single jet in the Atlantic section (Figures 2a and 2d) that transforms into well-separated subtropical and subpolar jets in June (Figure 2j). In contrast, a negative SNAO is preceded with split and weaker jets in the Atlantic sector in spring (Figures 2b and 2e) that are combined in June (Figure 2k). The seasonal evolution of the jet locations and intensity shown in Figure 2 are somewhat consistent with experiments using simplified dynamical models (e.g., O'Rourke & Vallis, 2016). The stronger March subpolar jet off the United States eastern coast associated with the positive SNAO (Figure 2j, pink curve in Figure 2l) is more favorable for long wave (wavenumber 1–5) generations by the barotropic instability due to the greater shear of the zonal flow. These long waves tend to diffuse the zonal wind meridionally, leading to deceleration at the center of the jet core and acceleration north and south of the jet core (O'Rourke & Vallis, 2016). This process drives the two jets further apart and pushes subpolar jet poleward. As a result, the subpolar and subtropical jets become well separated in June (Figure 2j, pink curve in Figure 2l). On the other hand, for the well-separated subpolar and subtropical jets in March associated with the negative SNAO (Figure 2k, blue curve in Figure 2l), long waves tend to decelerate the jet cores and accelerate the

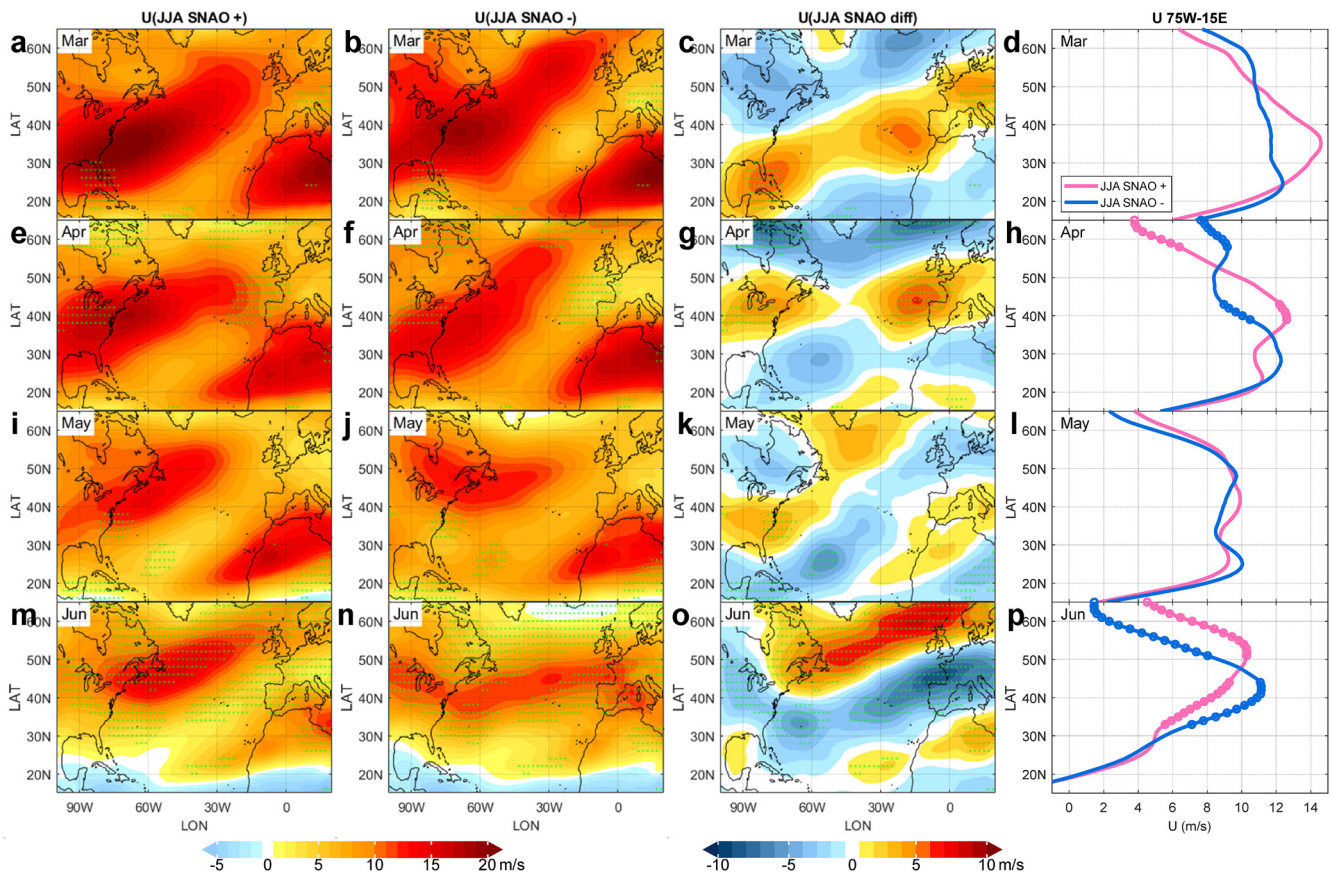


Figure 2. North-Atlantic zonal wind composites on summer North Atlantic Oscillation (NAO). The 1979–2018 March ERA5 tropospheric barotropic (100–1000 hPa) zonal wind composites with the June–July–August (JJA)–mean SNAO index (a), >1 , (b), <-1 , (c), their difference, and (d), the corresponding zonal wind composites averaged over 75°W–15°E. Same as (a–d), but for (e–h), April, (i–l), May, and (m–p), June zonal wind. Green dot-stippling in the first three column and the circles in the last column indicate that the local difference is significant at the 90% confidence level by a two-tailed *t*-test.

inter-jet region (O'Rourke & Vallis, 2016), driving the two jets closer in June (Figure 2b, blue curve in Figure 2c). Even though the jet structure evolution shown above does not contravene O'Rourke and Vallis (2016), their theory, however, cannot fully explain how the spring jet intensity and configurations are linked to the summer NAO. Further evidence shows below that stratosphere-troposphere coupling plays a critical role in the seasonal transition of the jet structure associated with SNAO.

Stratosphere-troposphere coupling has been considered a significant predictability source of surface climate, primarily in winter when polar stratospheric winds are strongly westerly (Baldwin & Dunkerton, 2001; Scaife et al., 2005; Thompson et al., 2002). It has not been widely applied to seasonal predictability in other seasons. We found here that the stratosphere-troposphere coupling remains active through the entire spring in the northern hemisphere extratropics and plays a critical role in the seasonal predictability of SNAO. Such predictability is realized mainly through localized vertical and meridional propagation of circulation anomalies over the North Atlantic region.

To determine how troposphere-stratosphere coupling may have contributed to the link between spring jet variability and SNAO, we show in Figure 3 the 31-day running average of the zonal wind averaged over the Atlantic sector as a function of height and latitude. The early March (representing the mean of the second half of February and the first half of March) North Atlantic zonal wind shows a positive (and statistically significant) surface anomaly below the center of the subtropical jet 3-month preceding a positive SNAO (Figure 3a). This zonal wind anomaly shifts northward and develops upward north of the subtropical jet core through mid-March and early April (Figures 3b and 3c). The negative-positive-negative anomaly in mid-March and early April acts to form a strong single jet in the upper troposphere and lower stratosphere (UTLS), as has been seen in Figures 2a

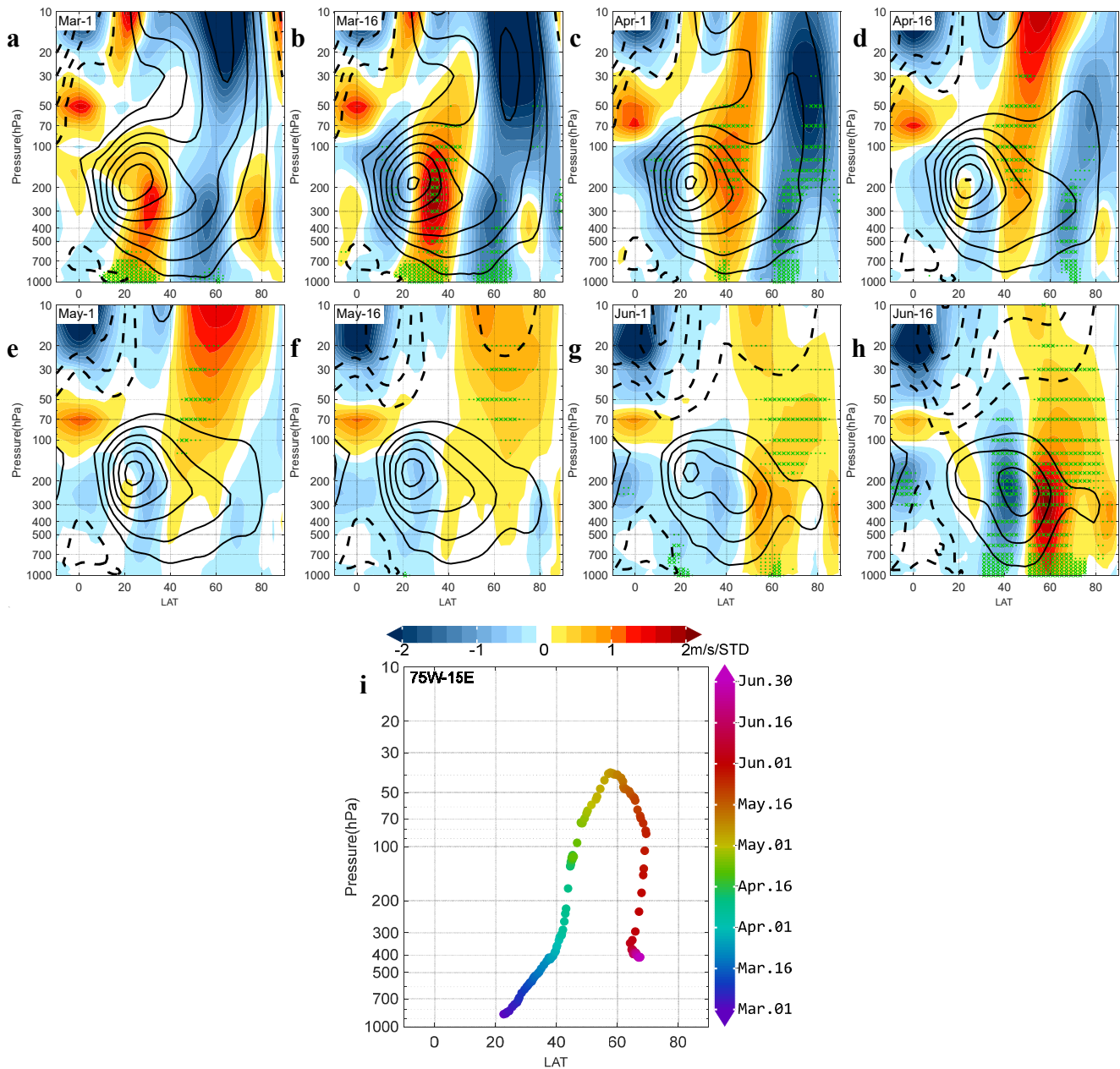


Figure 3. North-Atlantic zonal wind regressed on summer North Atlantic Oscillation (SNAO). The ERA5 1979–2018 31-day moving mean zonal wind averaged over 75°W–15°E regressed on the June–July–August (JJA)–mean SNAO index with central days on (a), March 1, (b), March 16, (c), April 1, (d), April 16, (e), May 1, (f), May 16, (g), June 1, and (h), June 16. (i), Mean locations of areas of positive wind anomaly significant at the 90% confidence level by a two-tailed t -test for all days from March 1 to June 30. Climatological zonal winds are overlaid in corresponding panels, with positive winds in solid contours, negative in dashed, and zero omitted, at an interval of 5 m s⁻¹. The green dot/cross-stippling in (a–h) indicates the 90%/95% confidence level by a two-tailed t -test, respectively.

and 2c. This single jet remains reinforced primarily in the mid-latitude UTLS in mid-April (Figure 3d). With the zonal wind anomaly decays in the troposphere in May, the reinforced mid-latitude lower stratospheric zonal wind starts to move poleward (Figures 3e and 3f). Once this positive wind anomaly reaches the northern high latitudes (Figure 3g), it extends downward to the troposphere and induces a deceleration on the equatorward flank of the subpolar jet (Figure 3h). As a result, the zonal wind anomaly associated with a positive SNAO drives the subpolar jet further northward, creating a double-jet structure (see also Figure 2j). The continuous evolution of the acceleration centers (Figure 3i) suggests an upward-poleward-downward propagation of the zonal wind anomaly from early spring to early summer. Through this process preceding a positive SNAO, the tropospheric zonal wind

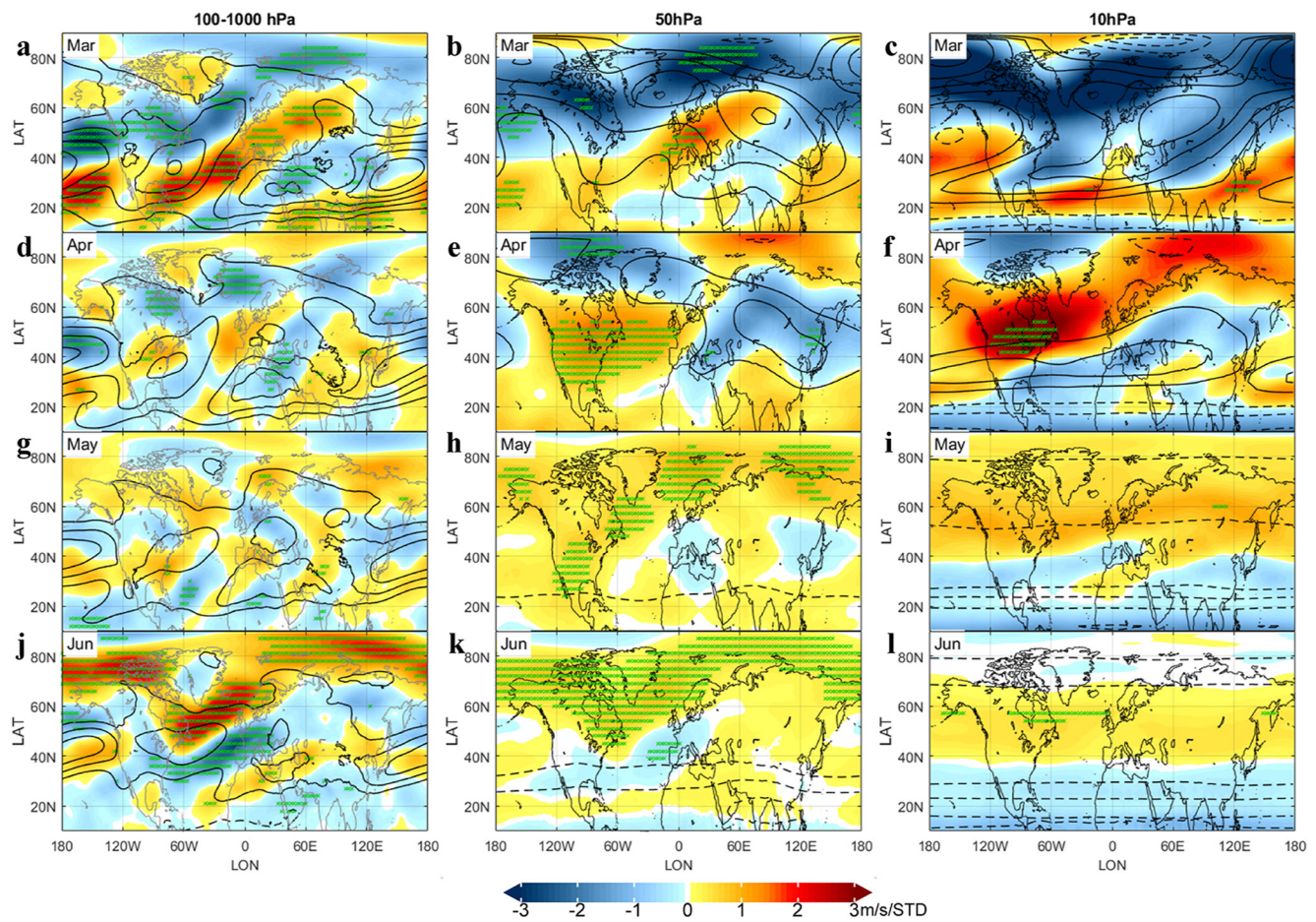


Figure 4. Monthly zonal wind regressed on summer North Atlantic Oscillation (SNAO). The 1979–2018 ERA5 (a), tropospheric (100–1000 hPa), (b), lower stratospheric (50 hPa), and (c), mid-stratospheric (10 hPa) zonal wind in March regressed on the June–July–August (JJA)–mean SNAO index. Same as (a–c), but for (d–f), April, (g–i), May, and (j–l), June zonal wind. Climatological zonal winds are overlaid in corresponding panels, with positive winds in solid contours, negative in dashed, and zero omitted, at an interval of 5 m s^{-1} . The green cross-stippling indicates the 95% confidence level by a two-tailed t -test.

evolved from a strong merged subtropical and subpolar jet in March (Figure 2a) to a northward shifted subpolar jet and a weak subtropical jet in June (Figure 2j).

Since O'Rourke and Vallis (2016) primarily focused on waves propagating meridionally between the tropospheric jets and found subordinate contribution from extra-long waves (wavenumber 1–2) that can penetrate into the stratosphere, their theory may not directly apply to the above troposphere-stratosphere-troposphere coupling processes. It thus calls for an additional explanation to these processes associated with SNAO. The March tropospheric barotropic zonal wind anomaly shows a negative-positive-negative tripolar pattern in the North Atlantic sector (Figure 4a), which reduces the zonal wind to the north and increases it to the south of the climatological jet location. The enhanced southwest-northeast-titled mid-latitude zonal wind is in favor of generating long waves that are easier to penetrate into the stratosphere than short waves, inducing wave-1 like zonal wind anomalies in the stratosphere in April (Figures 4e and 4f, one positive and one negative center across the longitudinal circle). In contrast, the April and May tropospheric zonal wind anomalies are rather erratic and distinct from their stratospheric counterpart, consisting of more wave-3 to 5 components (Figures 4d and 4g). The lower stratospheric zonal asymmetries interfere destructively with the climatological waves in April (shading vs. contours in Figures 4e and 4f). The reduced wave activity leads to weakened meridional residual circulation (Andrews et al., 1987; Kidston et al., 2015) and accelerated zonal wind on the poleward flank in May (Figures 4h and 4i), which can be illustrated by geopotential height anomaly associated with SNAO. The weakened meridional residual circulation causes a negative geopotential height anomaly in the polar stratosphere in May, extending down to the troposphere in June and persisting for the entire summer (stippled blue shading in Figure S3 in Supporting

Information S1). The negative geopotential height anomaly in the Arctic is dynamically consistent with the anomalously strong subpolar jet from the mid stratosphere to the troposphere in June (Figures 4j–4l), according to the thermal wind balance (Andrews et al., 1987). The June tropospheric barotropic zonal wind anomaly shows a positive-negative-positive tripolar pattern, opposite to that in March, in the North Atlantic sector (Figure 4j), indicative of a separated jet structure consistent with a positive SNAO. As visualized by the continuous propagation of zonal wind anomaly in Figure 3i and Figure S4 in Supporting Information S1, it is the troposphere-stratosphere-troposphere dynamical coupling that connects SNAO with the spring jet regime.

Based on the above relationship, the maximum strength of the mid-latitude barotropic zonal wind in the North Atlantic sector in March reflects the merging and splitting of the subtropical and subpolar jets and can thus serve as a predictor for SNAO. This March predictor shows a statistically significant and robust correlation with the JJA-mean SNAO index for all 20-year windows in the post-satellite era (Figure S5 in Supporting Information S1), making a skillful seasonal prediction of SNAO feasible months in advance. The March jet strength alone can predict SNAO with an anomaly correlation skill of 0.66 (Figure 1c; pink symbol in Figure S1a in Supporting Information S1). The skill can be further improved to 0.76 (blue symbol/curve in Figure S1a/S1c in Supporting Information S1) with two more March predictors, the eastern Indian Ocean rainfall and the North Atlantic sea surface temperature (SST). Adding an April predictor (the Pacific sea ice extent) boosts the skill to 0.81 (maroon symbol/curve in Figure S1a/S1c in Supporting Information S1), a level comparable to that of the winter NAO (Athanasiadis et al., 2017; Wang et al., 2017). However, this March-summer connection is primarily significant after the 1960s (Figure S6 in Supporting Information S1), possibly due to an unprecedented increase in atmospheric variability in recent several decades (Trouet et al., 2018).

5. Conclusions

The summer North Atlantic Oscillation has been long considered unpredictable due to the chaotic nature of the extratropical atmospheric circulation. Yet, the phase and amplitude of the summer North Atlantic Oscillation is crucial for the summer mean temperature and precipitation in the northern hemisphere as well as extreme heat-wave occurrences in many regions of Eurasia (Christidis et al., 2015; Sun, 2012). The discovery of the role of the stratosphere-troposphere coupling in this extended seasonal predictability indicates that the stratosphere-troposphere coupling has broader applications than previously thought. It also calls for the need to examine the relevant stratosphere-troposphere coupling processes in current dynamical models, as these models do not show any seasonal forecast skill in the summer North Atlantic Oscillation (Dunstone et al., 2018). Our findings that the summer North Atlantic Oscillation is highly predictable in the recent decades can enhance seasonal forecast skill of boreal summer climate and has great potential in applications in the energy and public health sectors.

Data Availability Statement

All the data used in this study are publicly available online. ERA-Interim and CERA20C are obtained from <https://apps.ecmwf.int/datasets/>, ERA5 from <https://cds.climate.copernicus.eu>, NCEP2 from <https://psl.noaa.gov/data/gridded/index.html>, MERRA2 from https://goldsmr5.gesdisc.eosdis.nasa.gov/data/MERRA2_MONTHLY/, JRA55 from <https://rda.ucar.edu/datasets/ds628.1/index.html>, and NOAA20CR from https://psl.noaa.gov/data/gridded/data.20thC_ReanV3.html.

References

- Andrews, D. G., Holton, J. R., & Leovy, C. B. (1987). *Middle atmosphere dynamics*. Academic Press.
- Athanasiadis, P. J., Bellucci, A., Scaife, A. A., Hermanson, L., Materia, S., Sanna, A., et al. (2017). A multisystem view of wintertime NAO seasonal predictions. *Journal of Climate*, 30(4), 1461–1475. <https://doi.org/10.1175/jcli-d-16-0153.1>
- Baker, H. S., Woollings, T., Forest, C. E., & Allen, M. R. (2019). The linear sensitivity of the North Atlantic Oscillation and eddy-driven jet to SSTs. *Journal of Climate*, 32(19), 6491–6511. <https://doi.org/10.1175/jcli-d-19-0038.1>
- Baldwin, M. P., & Dunkerton, T. J. (2001). Stratospheric harbingers of anomalous weather regimes. *Science*, 294(5542), 581–584. <https://doi.org/10.1126/science.1063315>
- Christidis, N., Jones, G. S., & Stott, P. A. (2015). Dramatically increasing chance of extremely hot summers since the 2003 European heatwave. *Nature Climate Change*, 5(1), 46–50. <https://doi.org/10.1038/nclimate2468>
- Collins, N., Theurich, G., DeLuca, C., Suarez, M., Trayanov, A., Balaji, V., et al. (2005). Design and implementation of components in the Earth system modeling framework. *International Journal of High Performance Computing Applications*, 19(3), 341–350. <https://doi.org/10.1177/1094342005056120>

Acknowledgments

The authors thank the European Centre for Medium-Range Weather Forecasts for providing ERA-Interim, CERA20C and ERA5 data, the Japan Meteorological Agency for JRA55, the NASA GSFC Global Modeling and Assimilation Office for MERRA2, the National Centers for Environmental Prediction for NCEP2, and the Physical Sciences Division at the National Oceanic and Atmospheric Administration and the Cooperative Institute for Research in Environmental Sciences at the University of Colorado Boulder for NOAA20CR. L. Wang is partially supported by grants 41875047 and 91837206 from National Natural Science Foundation of China (NSFC) and the Science and Technology Commission of Shanghai Municipality, China (20dz1200700). M. F. Ting is partially supported by NSF grant AGS 19-34258.

- Copernicus Climate Change Service (C3S). (2017). *ERA5: Fifth generation of ECMWF atmospheric reanalyses of the global climate*. Copernicus Climate Change Service Climate Data Store (CDS).
- Dee, D. P., Uppala, S. M., Simmons, A. J., Berrisford, P., Poli, P., Kobayashi, S., et al. (2011). The ERA-Interim reanalysis: Configuration and performance of the data assimilation system. *Quarterly Journal of the Royal Meteorological Society*, *137*(656), 553–597. <https://doi.org/10.1002/qj.828>
- Drouard, M., Kornhuber, K., & Woollings, T. (2019). Disentangling dynamic contributions to summer 2018 anomalous weather over Europe. *Geophysical Research Letters*, *46*(21), 12537–12546. <https://doi.org/10.1029/2019gl084601>
- Dunstone, N., Smith, D., Scaife, A., Hermanson, L., Eade, R., Robinson, N., et al. (2016). Skillful predictions of the winter North Atlantic Oscillation one year ahead. *Nature Geoscience*, *9*(11), 809–814. <https://doi.org/10.1038/ngeo2824>
- Dunstone, N., Smith, D., Scaife, A., Hermanson, L., Fereday, D., O'Reilly, C., et al. (2018). Skillful seasonal predictions of summer European rainfall. *Geophysical Research Letters*, *45*(7), 3246–3254. <https://doi.org/10.1002/2017gl076337>
- Folland, C. K., Knight, J., Linderholm, H. W., Fereday, D., Ineson, S., & Hurrell, J. W. (2009). The summer North Atlantic Oscillation: Past, present, and future. *Journal of Climate*, *22*(5), 1082–1103. <https://doi.org/10.1175/2008jcli2459.1>
- Franzke, C., & Woollings, T. (2011). On the persistence and predictability properties of North Atlantic climate variability. *Journal of Climate*, *24*(2), 466–472. <https://doi.org/10.1175/2010jcli3739.1>
- Gerber, E. P., & Vallis, G. K. (2009). On the zonal structure of the North Atlantic Oscillation and annular modes. *Journal of the Atmospheric Sciences*, *66*(2), 332–352. <https://doi.org/10.1175/2008jas2682.1>
- Hall, R. J., Scaife, A. A., Hanna, E., Jones, J. M., & Erdelyi, R. (2017). Simple statistical probabilistic forecasts of the winter NAO. *Weather and Forecasting*, *32*(4), 1585–1601. <https://doi.org/10.1175/waf-d-16-0124.1>
- Hurrell, J. (1995). *NAO index data provided by the climate analysis section*. NCAR. Retrieved from <http://www.cgd.ucar.edu/cas/jhurrell/indices.html>
- Hurrell, J. W., Kushnir, Y., Visbeck, M., & Ottensen, G. (2003). An overview of the North Atlantic Oscillation. In J. W. Hurrell, Y. Kushnir, G. Ottensen, & M. Visbeck (Eds.), *The North Atlantic Oscillation: Climatic significance and environmental impact, geophysical monograph series* (pp. 1–35). American Geophysical Union. <https://doi.org/10.1029/134gm01>
- Kanamitsu, M., Ebisuzaki, W., Woollen, J., Yang, S. K., Hnilo, J. J., Fiorino, M., & Potter, G. L. (2002). NCEP-DOE AMIP-II reanalysis (R-2). *Bulletin of the American Meteorological Society*, *83*(11), 1631–1644. <https://doi.org/10.1175/BAMS-83-11-1631>
- Kidston, J., Scaife, A. A., Hardiman, S. C., Mitchell, D. M., Butchart, N., Baldwin, M. P., & Gray, L. J. (2015). Stratospheric influence on tropospheric jet streams, storm tracks and surface weather. *Nature Geoscience*, *8*(6), 433–440. <https://doi.org/10.1038/ngeo2424>
- Kobayashi, S., Ota, Y., Harada, Y., Ebata, A., Moriya, M., Onoda, H., et al. (2015). The JRA-55 reanalysis: General specifications and basic characteristics. *Journal of the Meteorological Society of Japan*, *93*(1), 5–48. <https://doi.org/10.2151/jmsj.2015-001>
- Kutner, M. H., Nachtsheim, C. J., Neter, J., & Li, W. (2005). *Applied linear statistical models*. McGraw Hill Irwin.
- Lalouaux, P., de Boisseson, E., Balmaseda, M., Bidlot, J. R., Broennimann, S., Buizza, R., et al. (2018). CERA-20C: A coupled reanalysis of the twentieth century. *Journal of Advances in Modeling Earth Systems*, *10*(5), 1172–1195. <https://doi.org/10.1029/2018ms001273>
- O'Rourke, A. K., & Vallis, G. K. (2016). Meridional Rossby wave generation and propagation in the maintenance of the wintertime tropospheric double jet. *Journal of the Atmospheric Sciences*, *73*(5), 2179–2201. <https://doi.org/10.1175/JAS-D-15-0197.1>
- Scaife, A. A., Arribas, A., Blockley, E., Brookshaw, A., Clark, R. T., Dunstone, N., et al. (2014). Skillful long-range prediction of European and North American winters. *Geophysical Research Letters*, *41*(7), 2514–2519. <https://doi.org/10.1002/2014gl059637>
- Scaife, A. A., Knight, J. R., Vallis, G. K., & Folland, C. K. (2005). A stratospheric influence on the winter NAO and North Atlantic surface climate. *Geophysical Research Letters*, *32*(18), 109–127. <https://doi.org/10.1029/2005gl023226>
- Slivinski, L. C., Compo, G. P., Whitaker, J. S., Sardeshmukh, P. D., Giese, B. S., McColl, C., et al. (2019). Towards a more reliable historical reanalysis: Improvements for version 3 of the Twentieth Century Reanalysis system. *Quarterly Journal of the Royal Meteorological Society*, *145*(724), 2876–2908. <https://doi.org/10.1002/qj.3598>
- Sousa, P. M., Barriopedro, D., Ramos, A. M., Garcia-Herrera, R., Espirito-Santo, F., & Trigo, R. M. (2019). Saharan air intrusions as a relevant mechanism for Iberian heatwaves: The record breaking events of August 2018 and June 2019. *Weather and Climate Extremes*, *26*, 100224. <https://doi.org/10.1016/j.wace.2019.100224>
- Sun, J. Q. (2012). Possible impact of the summer north atlantic oscillation on extreme hot events in China. *Atmospheric and Oceanic Science Letters*, *5*(3), 231–234. <https://doi.org/10.1080/16742834.2012.11446996>
- Thompson, D. W. J., Baldwin, M. P., & Wallace, J. M. (2002). Stratospheric connection to Northern Hemisphere wintertime weather: Implications for prediction. *Journal of Climate*, *15*(12), 1421–1428. [https://doi.org/10.1175/1520-0442\(2002\)015<1421:sctnhw>2.0.co;2](https://doi.org/10.1175/1520-0442(2002)015<1421:sctnhw>2.0.co;2)
- Trouet, V., Babst, F., & Meko, M. (2018). Recent enhanced high-summer North Atlantic Jet variability emerges from three-century context. *Nature Communications*, *9*(1), 1–9. <https://doi.org/10.1038/s41467-017-02699-3>
- Wang, L., Ting, M., & Kushner, P. J. (2017). A robust empirical seasonal prediction of winter NAO and surface climate. *Scientific Reports*, *7*, 1–9. <https://doi.org/10.1038/s41598-017-00353-y>